

UNCLASSIFIED

Defense Technical Information Center
Compilation Part Notice

ADP013028

TITLE: Novel Cd[Se,Te]/BeTe Nanostructures: Fabrication by Molecular Beam Epitaxy and Properties

DISTRIBUTION: Approved for public release, distribution unlimited
Availability: Hard copy only.

This paper is part of the following report:

TITLE: Nanostructures: Physics and Technology International Symposium [8th] Held in St. Petersburg, Russia on June 19-23, 2000 Proceedings

To order the complete compilation report, use: ADA407315

The component part is provided here to allow users access to individually authored sections of proceedings, annals, symposia, etc. However, the component should be considered within the context of the overall compilation report and not as a stand-alone technical report.

The following component part numbers comprise the compilation report:

ADP013002 thru ADP013146

UNCLASSIFIED

Novel Cd(Se,Te)/BeTe nanostructures: fabrication by molecular beam epitaxy and properties

S. V. Ivanov[†], G. Reuscher[‡], T. Gruber[‡], T. Muck[‡], V. Wagner[‡], J. Geurts[‡],
A. Waag[‡], G. Landwehr[†], T. V. Shubina[†], N. A. Sadchikov[†], A. A. Toropov[†]
and P. S. Kop'ev[†]

[†] Ioffe Physico-Technical Institute, St Petersburg, Russia

[‡]Physikalisches Institut der Universität Würzburg, D-97074 Würzburg, Germany

Recently different II–VI wide-gap systems such as CdS/ZnS [1], CdTe/ZnTe [2], CdSe/ZnSe [3–5] have been tested for a possibility to fabricate quantum dot (QD) structures with high binding energy of zero-dimensional excitons, with the latter two systems being studied more intensively. Green RT lasers using as an active region a sheet of CdSe-based QD-like islands in a ZnSe matrix have been fabricated [6], demonstrating extremely low thresholds and enhanced degradation stability as compared to quantum well (QW) lasers. Typical features of all above mentioned QD systems are a common anion sublattice and, as a consequence, a type-I band alignment.

In this paper we report for the first time on fabrication by molecular beam epitaxy (MBE) and investigation of structural and optical properties of a new class of II–VI wide gap nanostructures based on ultra-thin CdSe insertions in a BeTe matrix, which have no common atoms at the CdSe/BeTe interface and are characterized by a type-II band structure and by the same lattice mismatch ($\sim 7\%$) as for the CdSe/ZnSe heteropair. It is expected that higher bond strength of BeTe can suppress significantly interdiffusion processes characteristic for CdSe/ZnSe [7] (like e.g. in ZnSe/BeTe multiple QWs [8]), as well as affect on the CdSe island formation mechanism by the intentional growing of highly strained BeSe or CdTe interfaces. Schematic band alignment diagram of the system is presented in Fig. 1.

Four CdSe/BeTe MQW structures have been grown on (100)GaAs substrates at 300°C by a conventional MBE mode in a Riber 2300 setup. A 5 monolayer (ML) thick BeTe buffer layer was initially grown at 350°C on a c(4×4) surface of a GaAs buffer layer. BeTe and CdSe growth rate gradients across the wafer and specular spot intensity (SSI) during the nanostructure growth were examined *in situ* by a specially designed RHEED system. Structural properties of the MQW structures were analysed using high resolution x-ray diffraction (XRD) measurements using a Philips X'pert diffractometer equipped with a four-crystal Ge 220 monochromator. Photoluminescence (PL) measurements were performed at 77 K and RT using 1 mW He-Cd (325 nm) and 2.5 mW Ar⁺ (457 nm) lasers.

All the structure parameters estimated from XRD and RHEED are summarized in Table.

Table.

Sample	CdSe nominal thickness, ML	1st interface	2nd interface	MQW period, nm	Number of periods
A	1.0	BeSe-0.5ML	BeSe-0.5ML	4.5	10
B	1.0	CdTe-SSI max.	CdTe-SSI 2nd min.	5.0	5
C	1.0	CdTe-SSI max.	CdTe-SSI max.	6.0	5
D	1.5	CdTe-SSI 1st min.	CdTe-SSI max.	6.0	10

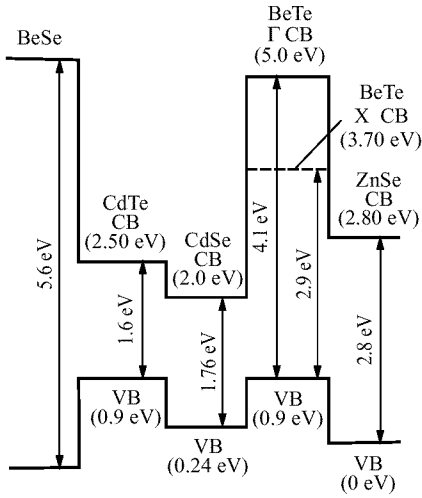


Fig. 1. BeSe-CdTe-CdSe-BeTe band alignment.

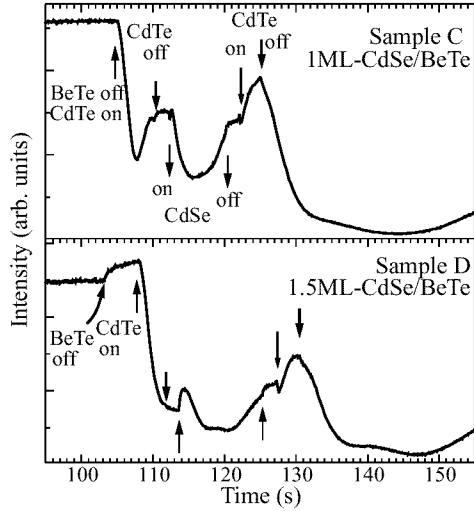


Fig. 2. RHEED specular spot intensity variation during growth of one MQW period of samples C and D.

Due to the huge lattice mismatch of the interface compounds with GaAs: -10 and $+15\%$ for BeSe and CdTe, respectively, their critical thickness should be below 1 ML. Therefore, fractional MLs of BeSe and especially CdTe, intentionally grown at a BeTe/CdSe interface, may serve as local *compressive or tensile stressors* for enforced CdSe nucleation on the BeTe surface. Sample A containing BeSe interfaces demonstrates a dramatic decrease in SSI during growth of both interfaces, which cannot be completely recovered by the following 1 ML CdSe and 4.5 nm BeTe layers. This results in disturbed structural quality and strongly suppressed PL intensity at 77 K.

The RHEED SSI variation during growth of one MQW period of samples C and D with CdTe interfaces are shown in Fig. 2. As has been observed in additional experiments which will be reported elsewhere, CdTe growth on BeTe involves three stages characterized by the specific SSI behavior: (i) an abrupt drop to a 1st SSI minimum likely corresponding to a maximum morphological and stress disorder introduced by pseudomorphically deposited CdTe, (ii) partial recovering and smoothing the interface, resulting in the intermediate SSI maximum, and (iii) final SSI reduction accompanied by a streaky to spotty RHEED pattern transformation indicating an onset of 3D growth. The whole SSI variation is limited by the CdTe thickness of ~ 0.5 ML (for strained CdTe), as estimated from XRD analysis of CdTe/BeTe MQWs. As is seen from Fig. 2, sample C has both CdTe interfaces corresponding to the SSI maximum (stage II), with CdTe nominal thickness being 0.25 and 0.15 ML, respectively, whereas the first CdTe interface in sample D is intentionally interrupted at SSI minimum (stage I), i.e. at ~ 0.15 ML. One should mention that sample B having the second CdTe interface slightly beyond the SSI maximum (~ 0.20 ML) shows gradual decrease in the integral SSI during the growth, resulting finally in poor structural quality and PL intensity. Contrary to that, the samples C and D demonstrate non-degraded SSI behavior during the whole structure growth, which is reflected in bright PL both at 77 and 300 K.

Figure 3 presents PL spectra of these samples in a logarithmic scale, taken at 77 K at

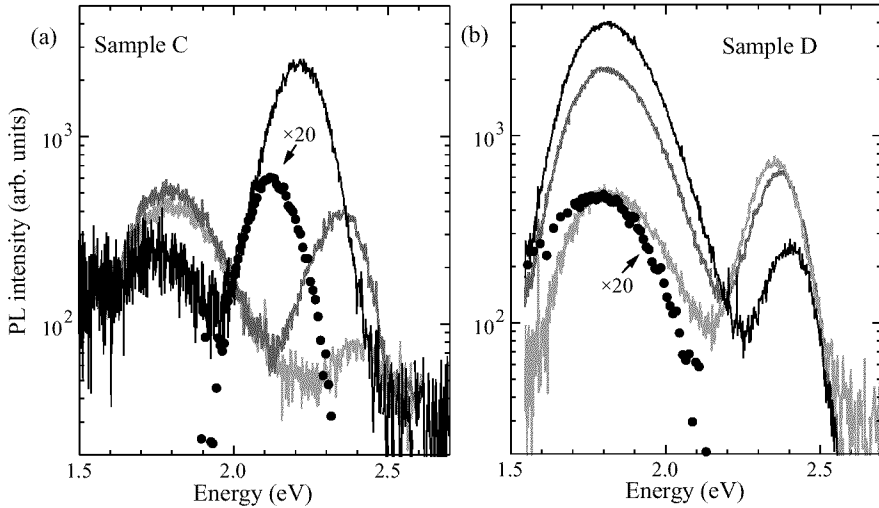


Fig. 3. PL spectra of samples C (a) and D (b), measured at 77 K at different points across the sample surface (solid lines) and at 300 K at the point with a maximum Cd flux (dotted lines). Total Cd flux decrease from black to grey and to light grey solid lines is estimated as 30%.

different points along the Cd gradient on the surface (solid lines) and at RT at the point with a maximum Cd(Se,Te) thickness (dotted line). The parameters presented in Table 1 for both structures also correspond to the point where Cd flux is maximal. Low temperature PL spectra of both samples involve two separated lines, with an integral PL intensity being much higher for sample D having larger CdSe thickness. The high-energy line dominating the spectra of sample C is narrower and shifts to blue between 2.2 and 2.45 eV with the CdSe thickness decrease, while the approximately twice broader low-energy band, dominant for sample D, is practically fixed at ~ 1.8 eV at any point on the sample surface. Additionally, strong redistribution of the PL intensity from high- to low-energy lines accompanies the Cd(Se,Te) thickness reduction for the sample C demonstrating also much larger blue shift of the high-energy line. Both of these effects are less pronounced in sample D, although they develop in a reverse direction versus Cd(Se,Te) thickness. A RT PL band in both structures follows the dominant lines, which may serve as an evidence of their intrinsic excitonic nature. However, further experiments, e.g. time resolved PL, are necessary to confirm this claim.

Summarizing these findings, the high-energy line can be assigned to a uniform Cd(Se,Te)/BeTe type-II QW, correlating well with the smooth 1st CdTe interface corresponding to the point with the maximum Cd flux (Fig. 2, sample C). The low-energy line is likely attributed to CdSe-based islands with a wide lateral size distribution. The dominance of this line in sample D agrees well with the highest non-uniformity of the 1st CdTe interface, stimulating the Cd(Se,Te) islands nucleation, at the point of maximum Cd flux related to the RHEED pictures in Fig. 2. A decrease in Cd amount along the sample surface obviously leads to a decay of integral PL intensity (from black to grey). Simultaneously, the 1st CdTe interface thickness also decreases, changing CdSe nucleation conditions. For sample C the reverse situation is observed. These speculations are additionally confirmed by XRD data presented for sample C in Fig. 4. The clearly observed MQW satellites and oscillation fringes strictly corresponding to the number of MQW periods indicate a high crystalline quality and uniformity of the Cd(Se,Te)/BeTe MQW structure, whereas the high

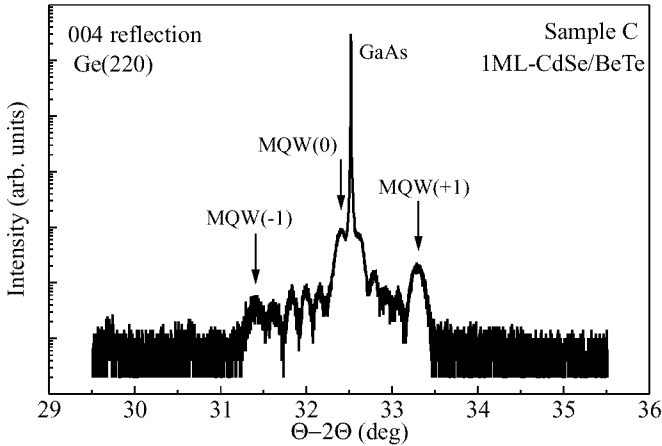


Fig. 4. $\Theta-2\Theta$ XRD rocking curve of sample C.

satellite intensity evidences a rather high compositional contrast in the MQW, i.e. less pronounced interdiffusion processes. Contrary to that, XRD data on sample D does not reveal the MQW satellites at all, which evidences the significantly disordered Cd(Se,Te) sheets.

In conclusion, CdSe/BeTe type-II nanostructures have been grown by MBE on GaAs substrates and studied by RHEED, XRD and PL for the first time. These structures demonstrate extremely high sensitivity to the interface bond type (BeSe or CdTe), with the CdTe interfaces providing much higher structural quality and PL intensity. Formation of the first CdTe interface, controlled by RHEED at the 0.1 ML level, causes radical variation of the structure morphology at a similar CdSe nominal thickness in the 1.0–1.5 ML range. It may be changed from the well defined homogeneous Cd(Se,Te) QW in the case of the smooth interface to the array of CdSe-based nanoislands (or QDs) coupled by much thinner QW in the case of non-uniform locally strained interface. However, final conclusion on the intrinsic morphology of these structures needs high resolution transmission electron microscopy studies, which are currently under the way.

Acknowledgements

This work was supported in part by RFBR, the Program of the Ministry of Sciences of RF “Physics of Solid State Nanostructures”, Volkswagen Stiftung and INTAS Grant No 97-31907.

References

- [1] W. Petri, *et al.*, *J. Cryst. Growth* **184/185**, 320 (1998).
- [2] P. Lefebvre, *et al.*, *Phys. Rev.* **B56**, 3097 (1997).
- [3] F. Flack, *et al.*, *Phys. Rev.* **B54**, 1731 (1996).
- [4] A. A. Toropov, *et al.*, *Jpn. J. Appl. Phys.* **38**, 566 (1999).
- [5] T. Kümmell, *et al.*, *Appl. Phys. Lett.* **73**, 3105 (1998).
- [6] S. V. Ivanov, *et al.*, *Appl. Phys. Lett.* **74**, 498 (1999).
- [7] R. N. Kyutt, *et al.*, *Appl. Phys. Lett.* **75**, 373 (1999).
- [8] Th. Walter, *et al.*, *Microscopy of Semiconducting Materials*, UK: IOP, Oxford, p 315, 1997.